

AD-A051 701

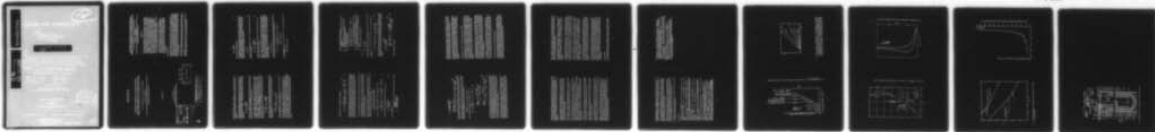
HARVARD COLL OBSERVATORY CAMBRIDGE MASS CENTER FOR AS--ETC F/6 20/5  
COMPARISON OF THEORETICAL AND OBSERVED HYDROGEN MASER STABILITY--ETC(U)  
DEC 77 R F VESSOT, M W LEVINE, E M MATTISON N00014-77-C-0777

UNCLASSIFIED

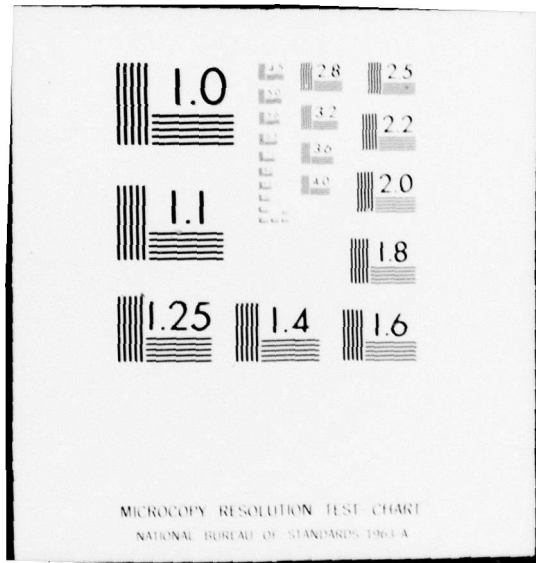
PREPRINT-895

NL

| OF |  
AD  
A051701



END  
DATE  
FILMED  
5 -78:  
DDC



12

AD A 051701

CENTER FOR ASTROPHYSICS

PREPRINT SERIES

Contract No. N00014-77-C-0777new

15

AD No.

DDC FILE COPY

RESEARCH ON SUBSTITUTION AND QUANTUM BEHAVIOR IN  
POLYMER SYSTEMS UNDER HIGH PRESSURE AND THE  
EFFECT OF TEMPERATURE ON LOW TEMPERATURE OPERATION

PREPRINT SERIES

1977

1977

DDC  
RECEIVED  
10 24 77  
REQUEST  
D

13

Center for Astrophysics  
Preprint Series No. 895

COMPARISON OF THEORETICAL AND OBSERVED HYDROGEN  
MASER STABILITY LIMITATION DUE TO THERMAL NOISE AND THE  
PROSPECT FOR IMPROVEMENT BY LOW-TEMPERATURE OPERATION

R. F. C. Vessot, M. W. Levine, and E. M. Mattison

Center for Astrophysics  
Harvard College Observatory and Smithsonian Astrophysical Observatory  
Cambridge, Massachusetts 02138

COMPARISON OF THEORETICAL AND OBSERVED HYDROGEN  
MASER STABILITY LIMITATION DUE TO THERMAL NOISE AND THE  
PROSPECT FOR IMPROVEMENT BY LOW-TEMPERATURE OPERATION

R. F. C. Vessot, M. W. Levine, and E. M. Mattison  
Center for Astrophysics  
Harvard College Observatory and Smithsonian Astrophysical Observatory  
Cambridge, Massachusetts 02138

ABSTRACT

Expressions describing the limitations to hydrogen maser stability due to random thermal noise are derived in terms of parameters that govern the operation of the maser oscillator. Possible effects from cavity pulling have been included by the ad hoc assumption of a random cavity resonance frequency variation characterized by a  $f^{-2}$  spectrum. The measured stability of the recently developed SAO VLG-11 masers is compared with the predicted stability limitations, and good agreement with theory is found for averaging times  $\tau$  between  $0.83 \text{ sec}$  and  $4.2 \times 10^3 \text{ sec}$ . The best observed Allan variance is  $\sigma(2, 4.2 \times 10^3, 4.2 \times 10^3, 6) = 6 \times 10^{-16}$ . For  $\tau > 4.2 \times 10^3 \text{ sec}$ , systematic variations appear to dominate the data, and the variance representation is no longer appropriate.

Using the stability limitation expressions ~~we analyzed~~ the consequences of low temperature maser operation. We find that if the wall relaxation probability per collision remains at or below its room temperature value, there is a high likelihood of substantial improvement in maser performance from operation at cryogenic temperatures.

INTRODUCTION

The invention of the atomic hydrogen maser by Kleppner, Goldenberg and Ramsey in 1930 resulted from a search for means of reducing the resonance linewidth of an atomic clock by increasing the unperturbed interaction time of atoms in the microwave field that causes resonance transitions. An additional attractive feature that stimulated the search was the possibility of operating an atomic frequency standard as a microwave self-oscillator as had been done by Townes and by Basov in their pioneering work<sup>2,3</sup> using the ammonia molecule as a maser oscillator.

Early results from the hydrogen maser indicated that storage times of about 1 sec could be realized by reflecting hydrogen atoms from surfaces coated with

This work is supported by NASA's George C. Marshall Space Flight Center and Jet Propulsion Laboratory and also by the Office of Naval Research.

December 1977

To be published in  
Proceedings for the Ninth Annual  
Precise Time and Time Interval Conference

D D C  
RECEIVED  
MAR 24 1978

SEARCHED	INDEXED	SERIALIZED	FILED
APR 1978			
FBI - NEW YORK			
REX file on file			
A			

DISTRIBUTION STATEMENT A  
Approved for public release;  
Distribution Unlimited

alkylchloro-silanes (Dri-Film) or with Teflon. By using this type of wall coating in the maser storage bulb, oscillator line Q's on the order of  $10^9$  were achieved.

Predictions of the stability of such high Q oscillators were made using traditional methods<sup>[1]</sup> that assume that instability is due mainly to thermal noise within the oscillator linewidth. These predictions indicated that the stability should vary as  $\tau^{-1/2}$ , where  $\tau$  is the averaging time interval, according to the expression

$$\frac{\Delta f}{f} = \frac{1}{Q_L} \sqrt{\frac{kT}{2P_b \tau}} \quad (1)$$

Here  $Q_L$  is the effective quality factor of the atomic resonance (the line  $Q$ ),  $P_b$  is the power delivered by the radiating atoms to the resonant cavity,  $k$  is the Boltzmann constant, and  $T$  is the absolute temperature.

Early measurements of maser stability<sup>[4]</sup> indicated that other noise processes completely overwhelmed the noise source described by equation (1). Cross-correlation tests<sup>[5]</sup> of maser signals showed that the major source of maser instability was additive white phase noise within the bandwidth of the receiving or measuring system. In general, this noise could be described as due to an r.m.s. phase deviation,  $\Delta\phi = \sqrt{(kT/B)P_0}$ , where  $F$  is the noise figure of the receiver,  $B$  is the effective noise bandwidth of the receiver, and  $P_0$  is the power input to the receiver. In terms of a frequency stability measurement over a time interval  $\tau$ , we have

$$\frac{\Delta f}{f} = \frac{\Delta\phi}{2\pi f \tau} = \frac{1}{2\pi f \tau} \sqrt{\frac{FkTB}{P_0}} \quad (2)$$

The two noise processes, one identified with noise energy whose spectral components lie within the oscillator linewidth and the other with noise energy lying within the bandwidth of the receiver, can be combined as uncorrelated processes<sup>[6]</sup> to give

$$\frac{\Delta f}{f} = \left[ \frac{kT}{2} \left( \frac{FB}{2\pi^2 f^2 P_0} + \frac{1}{Q_L^2 P_b \tau} \right) \right]^{1/2} \quad (3)$$

Note that a distinction is made here between the oscillator power level  $P_b$  and the power delivered to the receiver system,  $P_0$ .

As the development, building, and testing of hydrogen masers continued, the stability data<sup>[7]</sup> agreed fairly well with equation (3), but the stability plot almost invariably flattened out for long averaging times, becoming proportional to  $\tau^0$ . This behavior could be characterized by a spectral distribution known as flicker of frequency noise.<sup>[8]</sup> It appeared to be due to a combination of systematic effects chiefly associated with the maser's resonant cavity. Variations  $\Delta f_c$  in the cavity resonance frequency pull the maser output frequency by an amount

$$\Delta f_{out} = \frac{Q_L}{Q_f} \Delta f_c \quad (4)$$

where  $Q_L$  is the loaded cavity  $Q$ .

The statistical effect of such pulling can be included in the variance expression in equation (3) if we postulate that  $\Delta f_c$  can be assigned a spectral behavior to describe its frequency fluctuations. In view of the observed data the logical choice is to assume that  $\Delta f_c$  follows the  $1/f$  spectral law, and write the power spectral density of cavity frequency variations as

$$S_{f_c} = \frac{h_c}{f} \quad (5)$$

where  $h_c$  is a proportionality constant. We can thus express the power spectral density of the output as

$$S_{f(t)} = \frac{h_{-1}}{f} = \left( \frac{Q_L}{Q_f} \right)^2 \frac{h_c}{f} \quad (6)$$

If this spectral process is uncorrelated with the others, we can include it in expression (3) for the variance.

Before we do this it is appropriate to describe the variance in terms of the two-sample or Allan variance  $\sigma_f^2(2, T, \tau, B)$ , where  $\tau$  is, as before, the averaging interval,  $T$  is the time between the beginning of one such interval and the beginning of the next in a time-ordered progression of data, and  $B$  is the noise bandwidth of the receiver. For the case where  $T > \tau$ , i.e., there is "dead time" between data samples, and for the two types of noise processes represented by equation (3), we have

$$\sigma_f^2(2, T, \tau, B) = \frac{\Delta f}{f} \quad (7)$$

Since we desire to continue using the two-sample variance when we include the cavity flicker effect, we must represent the flicker variance  $\sigma_f$  as

$$\sigma_f^2(2, T, \tau, B) = \frac{h_{-1}}{2} \left[ -2 \left( \frac{T}{\tau} \right)^2 \ln \frac{T}{\tau} + \left( \frac{T}{\tau} + 1 \right)^2 \ln \left( \frac{T}{\tau} + 1 \right) + \left( \frac{T}{\tau} - 1 \right)^2 \ln \left( \frac{T}{\tau} - 1 \right) \right]$$

In our practice  $(T - \tau)/\tau = 0.83/\tau$  so that  $(T - \tau)/\tau < 0.01$  for  $\tau > 83$  sec and we can write approximately

$$\sigma_f^2(2, T, \tau, B) \approx h_{-1} 2 \ln 2$$

Thus for  $(T - \tau)/\tau \ll 1$  the total Allan variance is

$$\sigma^2(2T, T, B) \approx \left[ \frac{kT}{2} \left( \frac{FB}{2\pi^2 P_o \tau^2} + \frac{1}{2P_b \tau} \right) + b_c \frac{Q_L^2}{2} + 2 \ln 2 \right]^{1/2} \quad (7)$$

According to the above description, the  $\tau^{-1/2}$  behavior of  $\sigma$  can be observed if the  $b_c$  factor describing the cavity resonance frequency variations is sufficiently small. An example of this is shown in Figure 1, [8] where we see that improving the power level  $P_b$  degrades the line  $Q$  owing to spin-exchange relaxation and, for a given level of cavity instability the flicker floor, or  $\tau^{-1}$ , data can combine with the  $\tau^{-1}$  data in such a way as to obscure the  $\tau^{-1/2}$  behavior.

#### STABILITY EXPRESSED IN TERMS OF THE MASER OPERATING PARAMETERS

The foregoing discussion has dealt with the operation of the hydrogen masers in terms of overall parameters. We now look more closely at the behavior of the hydrogen maser and seek to optimize its performance for various applications by considering its internal parameters.

Figure 2 (after Kleppner et al. [10]) shows the relation between oscillation power  $P_b$  and atomic flux  $I$ . The functional relationship between flux and power depends on a parameter,  $q$ , a threshold flux,  $I_{th}$ , and a critical power level,  $P_c$ . These three parameters are defined as follows:

$$q = \frac{\hbar}{8\pi\mu_0} \frac{I_{tot}}{2} \left( 1 + \frac{\gamma_w}{\gamma_b} \right) \frac{V_c}{\eta V_b} \frac{\sigma_{se}(T) v_f(T)}{Q_L} \quad (8)$$

The value of  $q$  must be less than 0.172 for oscillation to occur.

$$P_b = \frac{\omega^2}{8\pi\mu_0} \frac{V_c}{2} \frac{1}{\eta Q_L} (\gamma_b + \gamma_w)^2 \left[ 2q^2 \left( \frac{I}{I_{th}} \right)^2 + (1-3q) \frac{I}{I_{th}} - 1 \right] \quad (9)$$

This assumes wall relaxation processes for which  $\gamma_{1w} = \gamma_{2w}$ .

$$I_{th} = \frac{\hbar V_c (\gamma_b + \gamma_w)^2}{4\pi\mu_0 Q_L \eta} \quad (10)$$

In these equations,

- $\omega = 2\pi f$ , where  $f$  is the hydrogen hyperfine separation transition frequency.
- $\hbar =$  Planck's constant/ $2\pi$ .
- $\mu_0 =$  the Bohr magneton.

$I_{total} =$  the total flux entering the bulb.  
 $I =$  the flux in the  $F=1$ ,  $m_F=0$  hyperfine sublevel of atomic hydrogen.

$\gamma_w =$  the wall relaxation rate for loss of phase coherence.  
 $\gamma_b =$  the loss rate of atoms from the bulb.  
 $V_c =$  the resonant cavity volume.  
 $V_b =$  the storage bulb volume.

$\eta = \frac{(H_z \text{ averaged over bulb volume})^2}{H^2 \text{ averaged over the cavity volume}} =$  "filling factor"

where  $H$  is the rf magnetic field strength in the cavity and  $H_z$  is its component along the  $z$  axis.

$\sigma_{se}(T) =$  the spin exchange cross section, which depends on the speed of interatomic collisions and therefore on temperature.

$v_f(T) =$  the average relative velocity of the hydrogen atoms in the bulb.

$Q_L =$  the loaded  $Q$  of the cavity resonator.

We have

$$\frac{1}{Q_L} = \frac{1}{Q_0} + \frac{1}{Q_{ext}}$$

where  $Q_0$  is the unloaded  $Q$  of the resonator and  $Q_{ext}$  represents the loading due to the external circuitry coupled to the cavity.

We can express the line  $Q$  in terms of the parameter  $q$  and the beam flux as follows:

$$Q_L = \frac{\omega}{2\gamma} = \frac{\omega}{2(\gamma_b + \gamma_w + \gamma_{se})} = \frac{\omega}{2(\gamma_b + \gamma_w) \left( 1 + q \frac{1}{I_{th}} \right)} \quad (11)$$

where  $\gamma_{se}$  is the relaxation rate due to spin exchange. If we substitute the above expressions for  $Q_L$ ,  $P_b$ , and  $I_{th}$  into the stability expressions given in equations (1), (2), and (3), we have for the noise limit due to noise within the oscillation linewidth

$$\sigma_o = \frac{\Delta f}{f} = \frac{1}{Q_L} \left( \frac{1}{2} \frac{kT}{P_b} \right)^{1/2} = \left[ \frac{16\pi kT}{\omega^3} \frac{\mu_0 \eta}{\eta^2 V_c} \frac{Q_L}{\tau} \frac{1}{-1 + (1-3q) \frac{I}{I_{th}} - 2q^2 \left( \frac{I}{I_{th}} \right)^2} \right]^{1/2} \quad (12)$$

and for the additive noise limit

$$\sigma_s = \frac{1}{\omega \tau} \left( \frac{F K T B}{P_b} \frac{Q_{\text{ext}}}{Q_L} \right)^{1/2} \left\{ \frac{8\pi F K T B \gamma}{\omega^2 \tau^2 V_c} \frac{Q_{\text{ext}}}{(N_b + \gamma_b)^2} \frac{1}{2} \left[ -1 + (1 - 3q) \frac{1}{L_{\text{th}}} - 2q^2 \left( \frac{1}{L_{\text{th}}} \right)^2 \right] \right\}^{1/2} \quad (13)$$

These relations allow us to relate the stability limit to the operating conditions of the maser and to optimize the stability for a given averaging time interval  $\tau$ .

In addition to the thermal noise terms we can, as before, include the systematic effect of cavity mistuning if we characterize the mistuning by a flicker-of-frequency behavior. Substituting for  $Q_L$  in equation (6) we have

$$\sigma_f = \frac{2Q_L}{\omega} (N_w + \gamma_b) (1 + q V/L_{\text{th}})^2 (b_c 2 \ln 2)^{1/2}$$

and the complete expression for the stability is given by

$$\sigma(\tau, T, B) = \left\{ \frac{Q_L^2}{\omega^2} 4(N_w + \gamma_b)^2 (1 + q V/L_{\text{th}})^2 b_c 2 \ln 2 \tau^0 + \frac{16\pi K T}{\omega^2 \tau^2 V_c} \frac{V_0 \gamma Q_L (1 + q \frac{1}{L_{\text{th}}})^2}{-1 + (1 - 3q) \frac{1}{L_{\text{th}}} - 2q^2 \left( \frac{1}{L_{\text{th}}} \right)^2} \tau^{-1} + \frac{8\pi K T}{\omega^2 \tau^2 V_c} \frac{F Q_{\text{ext}} B}{(N_b + \gamma_b)^2 [-1 + (1 - 3q) \frac{1}{L_{\text{th}}} - 2q^2 \left( \frac{1}{L_{\text{th}}} \right)^2]} \tau^{-2} \right\}^{1/2} \quad (14)$$

This expression, which relates the statistical behavior of the maser's stability to its internal operating parameters, contains a great deal of information and gives a considerable amount of insight to the compromises and tradeoffs that must be considered in designing a device for a given application. For example if we choose an operating point by fixing  $q$  and  $V/L_{\text{th}}$  we see that the value of  $(N_w + \gamma_b) = \tau$  chosen for a particular design affects the  $\tau^0$  portion of  $\sigma$  as  $\tau$ , the  $\tau^{-1/2}$  portion as  $\tau^{-1}$ , and the  $\tau^{-1}$  portion as  $\tau^{-1}$ . The tradeoff between short-term and long-term stability is very evident here.

The appearance in equation (14) of  $Q_{\text{ext}}$  the external loading  $Q_e$  and of  $Q_L$  the loaded cavity  $Q$ , also is of considerable interest. At first glance it would appear that we should make  $Q_e$  the intrinsic cavity  $Q$ , as high as possible, then make  $Q_L$  and  $Q_{\text{ext}}$  as low as possible by overcoupling. However, if we look more critically we see that heavy external loading can be harmful because the cavity resonance frequency (which necessarily depends on  $Q_{\text{ext}}$ ) can be

shifted by such effects as line variations owing to temperature or by variations in the input impedance of the receiver. The fact that  $Q_L$  appears in the  $\tau^0$  portion of the stability function as  $Q_L^2$  may tempt us to reduce  $Q_L$  by loading the cavity heavily, but systematic effects can negate any such benefits.

We have arbitrarily added the effect of cavity pulling in the stability equation to illustrate the effect of line  $Q$  in competition with the cavity  $Q$ ; there is no physical reason that the cavity effect will have the assigned flicker-like behavior. Furthermore, if cavity perturbations can be reduced, it should be possible to see the underlying  $\tau^{-1/2}$  behavior of  $\sigma$  due to thermal noise within the oscillator linewidth.

#### COMPARISON OF VLG-11 STABILITY DATA WITH THEORY

During the past summer we have had the opportunity to make measurements on the newly developed VLG-11 masers<sup>11, 12</sup> that were described at last year's P. T. I. conference. The sensitivity of the maser to magnetic, thermal, and barometric variations have been reported elsewhere;<sup>11, 12</sup> there is no measurable barometric effect and the sensitivity to temperature and magnetic fields have been diminished by a factor of approximately 3 from the previous VLG-10A design used as ground station equipment for the 1976 gravitational redshift mission.

The stability data obtained from the VLG-11 tests are shown in Figure 3 along with the operating parameters for the test. The stability data closely follow the theoretical limit for averaging intervals from 0.83 sec to 1 hr. The best stability is  $\sigma(2, 4.2 \times 10^3, 6) = 6 \times 10^{-16}$ . For  $\tau > 4.2 \times 10^3$  the statistical representation of the data shows the evidence of the slow drift that seemed to be the result of incomplete thermal stabilization of the masers and of variations in the laboratory temperature. Representing such systematic effects by a statistical variance is inappropriate.

The stability for  $\tau < 1$  hr is limited by thermal noise. Perhaps it could be improved by operating the maser at more nearly optimum conditions, but we believe the improvement would not be a large one. Clearly, if a major improvement is to be made it will have to be the result of a substantial change in the parameters in equation (14) that describe the operating condition of the maser.

#### SPECULATION ON THE COLD HYDROGEN MASER

Recently the preliminary results of experiments on cold atomic hydrogen by Professor Daniel Kleppner and his co-workers at the Massachusetts Institute of Technology were brought to our attention by Professor Irwin Shapiro, who suggested that these data might offer new insights to hydrogen maser development. Kleppner and his co-workers found that atomic hydrogen could be stored as a gas at 4 K even though molecular hydrogen freezes at 14 K.

It appears that the retention of atomic hydrogen is made possible by the presence of a coating of frozen molecular hydrogen on the walls of the storage vessel. If such a coating became contaminated with impurity atoms, atomic hydrogen would recombine on the impurity sites to form H<sub>2</sub>, thus renewing the continuous hydrogen film. This would be an attractive property for a hydrogen maser storage bulb.

To illustrate the behavior of a cold hydrogen maser, we must establish a set of oscillation conditions. We can fix an operating point in Figure 2 by holding  $q$  and  $1/4$ th constant as we lower the temperature. In this example we will also keep the cavity and bulb dimensions constant and assume that the wall relaxation probability remains unchanged.

The parameter  $q$  contains two temperature-dependent terms, the spin-exchange cross section,  $\sigma_{se}$ , and the average relative velocity,  $v_r$ . The dependence of  $\sigma_{se}$  on temperature is given by Allison [14] and is shown in Figure 4.

If we lower the temperature from 322 K to 4 K, we see that  $\sigma_{se}$  decreases by a factor of about 22 and the velocity decreases by the factor  $\sqrt{322/4} = 9$ . The ratio  $[\sigma_{se}(322) v_r(322)] / [\sigma_{se}(4) v_r(4)]$  is about 198, so in order to keep  $q(322 \text{ K}) = q(4 \text{ K})$ , we can decrease  $Q_L$  by a factor of 198. In practice this would be done by overcoupling the cavity so that  $Q_{ext}(4 \text{ K}) \ll Q_0(4 \text{ K})$ . If, for example,  $Q_L(322 \text{ K}) = 3.5 \times 10^4$ , we find that  $Q_L(4 \text{ K})$  should be made about  $(3.5 \times 10^4) / 198 = 177$ , and  $Q_{ext} = 177$ . That the system should oscillate with such a remarkably low cavity  $Q$  is due to the long storage time produced by the low temperature.

Cooling the maser will also affect  $Q_f$  and from the right-hand side of equation (11) we see that if we keep  $1/4$ th unchanged  $Q_f$  will increase by the ratio  $\sqrt{322/4}$ , since both  $v_b$  and  $v_w$  are proportional to velocity and, hence, to  $T^{1/2}$ .

The pulling effect  $\Delta f_{out} = (Q_L \Delta f_0) / Q_f$ , which is the chief source of systematic drift in the maser, is reduced by a factor of  $1776 = 198 \times \sqrt{322/4}$ , since  $Q_f$  is improved and  $Q_L$  is reduced.

In order to maintain the operating point we must keep  $1/4$ th constant. The quantity  $1/4$  depends on the ratio  $(v_b + v_w)^2 / Q_L$ . At 4 K this quantity increases by a factor of  $198/80 = 2.5$ , which means that we must increase the atomic hydrogen flux by this amount in order to meet the conditions for our comparison.

Figure 5 shows the projected improvement in the stability limit under the above conditions. In this example we assume that the receiver noise figure  $F$  improves from 6 to 2 (7.5 db to 3 db) because the receiver's low noise preamplifier is considered to be at the same low temperature as the maser. The output power level depends on  $(v_b + v_w)^2 / Q_L$  and, under the assumptions of this example, is seen to increase by the factor  $198/\sqrt{322/4} \approx 22$  or 13 db. Based on the comparison with the actual SAO VLG-11 maser data, [12] we could expect an output power level of -85 dbm.

Maser operation at low temperatures leaves open other possibilities for improvement resulting from such phenomena as the reduction of thermal coefficients of expansion, the possibility of superconducting circuitry (including the cavity), and the use of superconducting magnetic shields.

As mentioned earlier, the big question is whether or not the hydrogen atom will successfully bounce off a frozen molecular hydrogen wall (or, if necessary, some other type of wall not yet specified). The wall relaxation term,  $\chi_w = v/\lambda p$ , contains  $p$ , the probability per collision of atomic relaxation by loss of phase coherence.

At present, the only data we know of that relate  $p$  to temperature are due to M. Desaintfucien, [15] Figure 6 (from ref. 15) shows the relaxation probability per bounce for a F. E. P. Teflon-coated bulb. These data show a slight decrease in  $p$  as temperature is decreased to 76 K. Whether or not the probability stays reasonably low as we go from 76 K to 4 K is a very important question, as is the question of the magnitude and stability of the wall shift at these low temperatures.

To test the feasibility of low-temperature operation, we have begun a program to construct a maser that will operate at low temperatures. Figure 7 is a schematic view of our planned apparatus. The dewar that houses the TE 111 mode cavity assembly [16] has an inside diameter of 7" and is enclosed in a set of magnetic shields. The first tests will be made at the boiling point of liquid nitrogen (~77 K) to verify that we can reproduce Desaintfucien's results for F. E. P. Teflon wall coatings.

We will then bring the dewar to liquid helium temperature while continuing pulsed operation and carefully monitoring the temperature of the cavity as it is cooled past 20 K, the condensing point of hydrogen, and 14 K, the freezing point of hydrogen. Successful pulsed operation below these temperatures will verify the storage of spin-aligned atomic hydrogen and will be a critical test of the device.

To prevent impurity atoms from reaching the interior of the cavity, a carefully located beam stop will be placed at the exit of the state selector magnet. At 4 K the cryostat itself becomes an extremely effective vacuum pump that will scavenge, by condensation and freezing, all stray gas other than helium in the system. The cavity assembly, by virtue of its thermal lag, will stay relatively clean until it, in turn, cools and condenses gas. It will then be possible to introduce in a controllable way gases such as argon or H<sub>2</sub> to serve as frozen-on wall coatings, and to observe the effect of these coatings on the relaxation rate of the hydrogen.

## CONCLUSIONS

The relationship of the maser oscillation parameters to the ultimate stability of masers provides considerable insight into the behavior of masers. Further

work would be useful. A systematic parametrization of maser performance can be made using computer techniques, and a more general treatment of wall relaxation can be made by eliminating the requirement made here that  $\gamma_{1w} = \gamma_{2w}$ .

It must be recognized that our approach is valid only for stochastic processes such as thermal noise. Systematic limitations of known origin can be included if the perturbation has a reasonably well understood spectrum, even though the physical basis for the spectrum is in question.

Whether or not the cold maser will work can only be determined by experiment and we look forward to observing the behavior of the maser as temperature is decreased. The prospect for making relativity measurements such as tests for gravity waves using precise intersatellite doppler measurements would be very much improved if stability in the  $10^{-7}$  level can be demonstrated.

We would like to thank Drs. D. Kleppner, S. Crampton, and I. Shapiro of M.I.T. for many useful and interesting discussions.

#### REFERENCES

- 1 Kleppner, D., H. M. Goldenberg, and N. F. Ramsey. Phys. Rev., vol. 126, No. 2, pp. 603-615 (1962).
- 2 Gordon, J. P., H. J. Zeiger, and C. H. Townes. Phys. Rev., vol. 95, p. 282, (1954).
- 3 Basov, N. G. and A. M. Prokhorov. J. Expl. Theoret. Phys. (U.S.S.R.), vol. 27, p. 431 (1954).
- 4 Vessot, R. F. C. Proc. 3rd International Conference on Quantum Electronics (Paris), Grivet and Bloembergen, eds., Columbia University Press, N. Y., pp. 409-417 (1963).
- 5 Vessot, R., L. Mueller, and J. Vanier. Proc. I.E.E.E., vol. 54, No. 2, pp. 199-207 (1966).
- 6 Cutler, L. S., and C. L. Searle. Proc. I.E.E.E., vol. 54, No. 2, pp. 136-154 (1966).
- 7 Finale, C., R. Sydnor, and A. Sward. Proc. 25th Frequency Control Symposium, U.S. Army Electronics Command, Ft. Monmouth, New Jersey, pp. 343-351 (1971).
- 8 Barnes, J. A. et al. IEEE Trans. Instr. Meas., vol. IM-20, No. 2, pp. 105-120 (1971).
- 9 Vessot, R. F. C., M. W. Levine, P. W. Zitzewitz, P. Debely, and N. F. Ramsey. In Precision Measurement and Fundamental Constants, D. N. Langenberg, ed., N. B. S. Special Publication No. 343, pp. 27-37 (1971).
- 10 Kleppner, D., S. B. Crampton, N. F. Ramsey, R. F. C. Vessot, H. Peters, and J. Vanier. Phys. Rev., vol. 139, No. 4A, pp. A972-A983 (1966).
- 11 Levine, M. W., R. Vessot, E. Mattison, T. Hoffman, G. Nyström, D. Graveline, R. Nicoll, C. Dovidio, and W. Brymer. In Proc. 8th Annual Precise Time and Time Interval (P. T. T. I.) Applications and Planning Meeting, U.S. Naval Research Laboratory, Wash., D. C., pp. 249-276 (1976).

- 12 Levine, M. W., R. Vessot, E. Mattison, G. Nyström, T. Hoffman, and E. Blomberg. A new generation of SAO hydrogen masers. Proc. 31st Annual Frequency Symposium on Frequency Control, U.S. Army Electronics Command, Ft. Monmouth, New Jersey, pp. 525-534 (1977).
- 13 Vessot, R. F. C., M. W. Levine, and E. M. Mattison. A report on the evaluation of the performance of the Smithsonian Astrophysical Observatory VLG-11 atomic hydrogen masers. Smithsonian Astrophysical Observatory, Cambridge, Mass. (November 1977).
- 14 Allison, A. C. Phys. Rev. A, vol. 5, No. 6, pp. 2695-2696 (1972).
- 15 Desaintfusquen, M. Ph.D. Thesis, University of Paris (1975).
- 16 Mattison, E. M., M. W. Levine, and R. F. C. Vessot. New TE 111 mode hydrogen maser. In Proc. 8th Annual Precise Time and Time Interval (P. T. T. I.) Applications and Planning Meeting, U.S. Naval Research Laboratory, Wash., D. C., pp. 355-367 (1976).

Fig. 1 - Relationship of short- and long-term stability as storage parameter  $\gamma$  is varied in the hydrogen maser (from ref. 9).

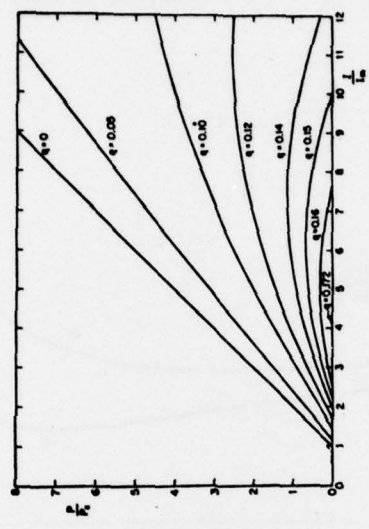
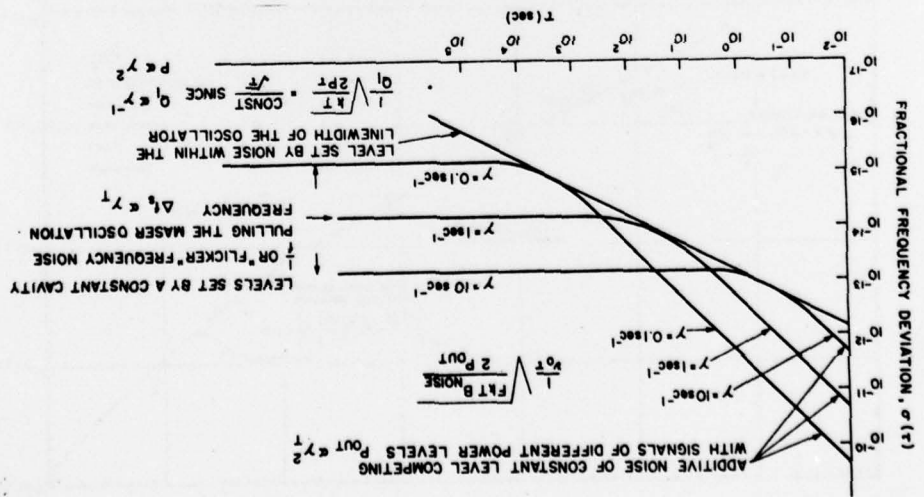


Fig. 2 -  $P/P_c$  versus  $1/\lambda$  for different values of the parameter  $q$ . This family of curves shows the strong influence of  $q$  on the operating conditions. If spin exchange is neglected,  $q=0$  and radiated power increases monotonically with beam flux. For  $q>0$  there is an upper limit to the flux for oscillation to occur and above a certain value ( $q=0.172$ ) the maser cannot oscillate at any beam flux,  $q$  is defined in Eq. (6) (from ref. 10).

Fig. 4—Dependence of spin exchange cross section on temperature (from ref. 14).

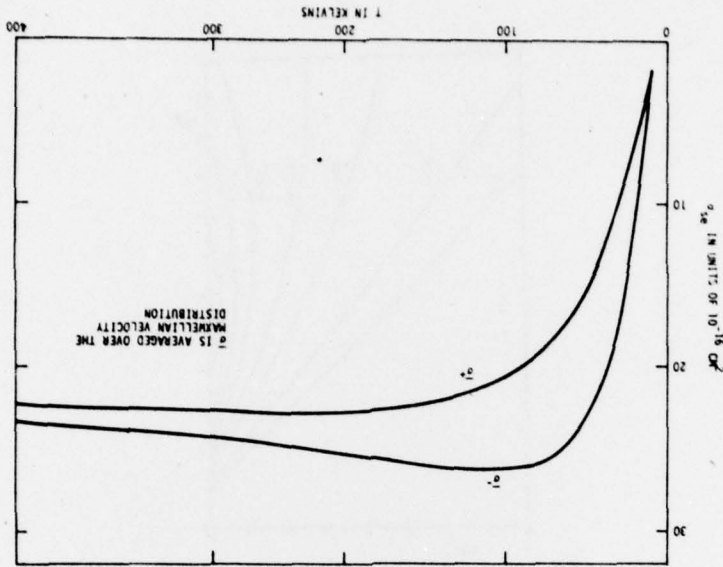
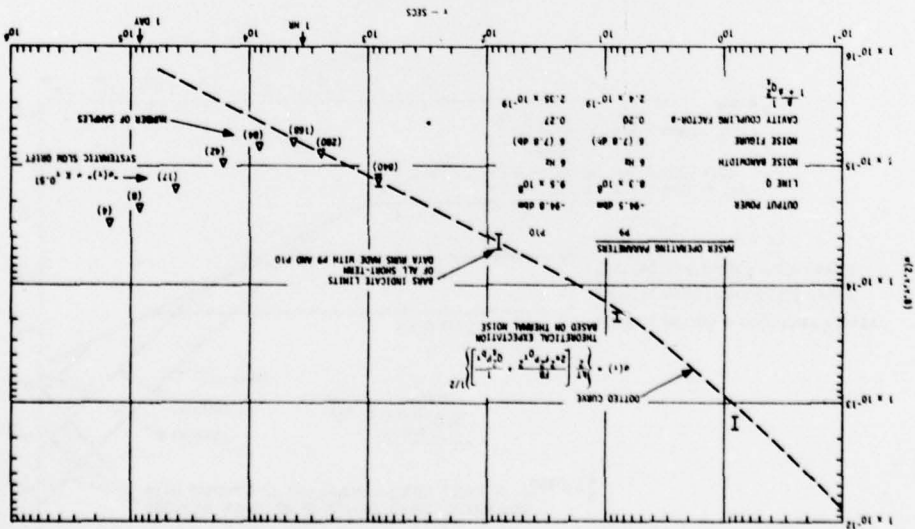


Fig. 3—VLC-11 stability data.  $\sigma(T_2, T_1, B)$  vs  $\tau$  for masers P9 and P10, October 9-17, 1977.



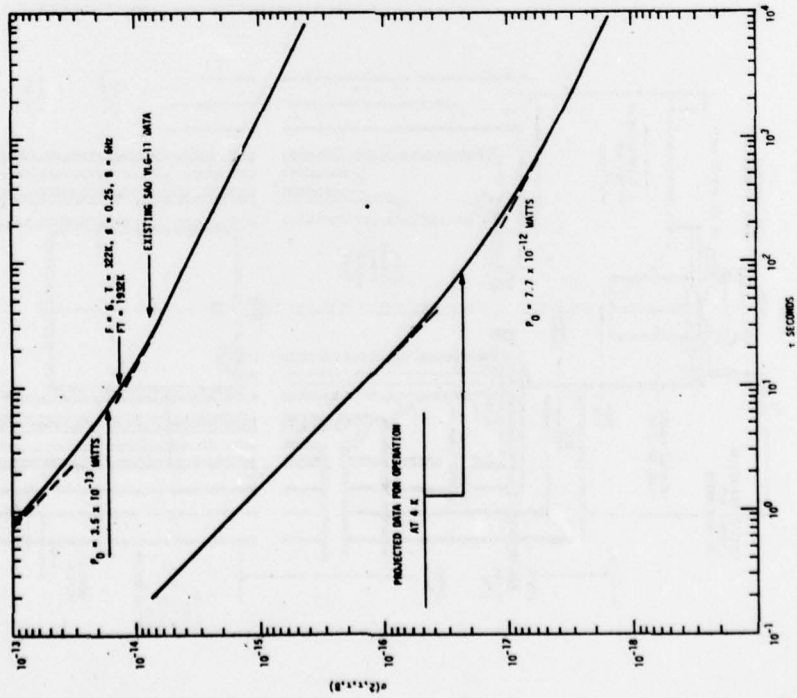
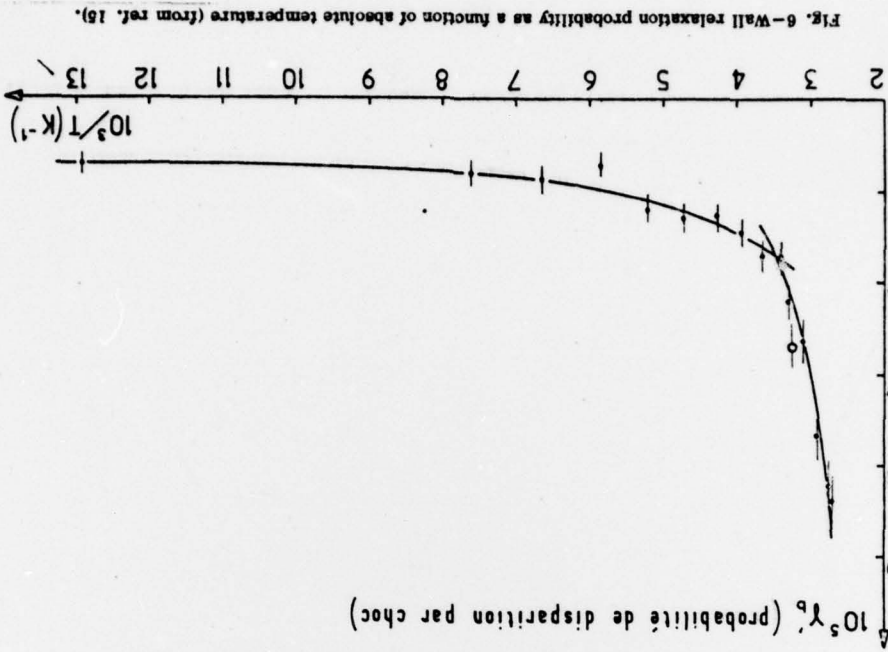


Fig. 5—Projected improvements in hydrogen-maser stability due to low-temperature operation.

Fig. 6—Wall relaxation probability as a function of absolute temperature (from ref. 15).

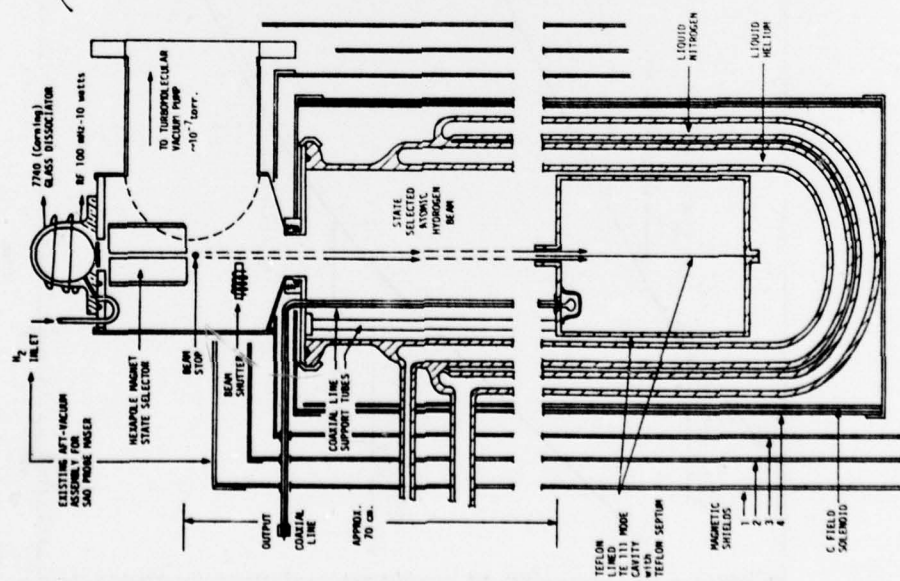


Fig. 7 - Schematic view of low-temperature atomic hydrogen maser.